



A comparison of soil water infiltration models of moisture irrigation

Binnan Li, Lixia Shen, Shuhui Liu

Publisher's Disclaimer

E-publishing ahead of print is increasingly important for the rapid dissemination of science. The *Early Access* service lets users access peer-reviewed articles well before print/regular issue publication, significantly reducing the time it takes for critical findings to reach the research community.

These articles are searchable and citable by their DOI (Digital Object Identifier).

Our Journal is, therefore, e-publishing PDF files of an early version of manuscripts that undergone a regular peer review and have been accepted for publication, but have not been through the typesetting, pagination and proofreading processes, which may lead to differences between this version and the final one.

The final version of the manuscript will then appear on a regular issue of the journal.

Please cite this article as doi: 10.4081/ija.2024.2216

 ©The Author(s), 2024
Licensee [PAGEPress](#), Italy

Submitted: 15/08/2023

Accepted: 23/02/2024

Note: The publisher is not responsible for the content or functionality of any supporting information supplied by the authors. Any queries should be directed to the corresponding author for the article.

All claims expressed in this article are solely those of the authors and do not necessarily represent those of their affiliated organizations, or those of the publisher, the editors and the reviewers. Any product that may be evaluated in this article or claim that may be made by its manufacturer is not guaranteed or endorsed by the publisher.

A comparison of soil water infiltration models of moisture irrigation

Binnan Li, Lixia Shen, Shuhui Liu

College of Water Conservancy and Engineering, Taiyuan University of Technology, Taiyuan, China

Correspondence: Lixia Shen, College of Water Conservancy and Engineering, Taiyuan University of Technology, Taiyuan 030024, China.

E-mail: shenlixia@tyut.edu.cn

Key words: Kostiakov model; GA-BP; PSO-SVM.

Contributions: BL, edited the draft; LS, SL, reviewed and edited the draft. All authors have read and approved the final version to be published.

Conflict of interest: the authors declare no potential conflict of interest.

Funding: this research was supported by the Basic Research Program of Shanxi Province (202103021224093;202103021224118).

Availability of data and material: the datasets used and/or analyzed during the current study are available from the corresponding author on reasonable request.

Abstract

As a water-saving method, moistube irrigation has been widely used. To ensure the effectiveness of moistube irrigation the development of an infiltration prediction model under moistube irrigation based on the interaction of multiple factors is required. In this paper, soil water infiltration tests with different bulk densities (1.2 g/cm³, 1.3 g/cm³, and 1.4 g/cm³) and textures (loamy sand, sandy loam, and clay loam) under different pressure heads (1m, 1.5m, and 2m) were designed, and the test data were analyzed by gray correlation theory. The pressure head, bulk density, clay content, silt content, sand content, and initial water content were determined as input variables, and the model structure was composed with two parameters of Kostikov's model as output variables. Then, the genetic algorithm was used to optimize the back propagation neural network and the particle swarm algorithm to optimize the support vector machine. The soil moisture prediction model under moistube irrigation was established, finally the model was compared and analyzed. The results showed that the consistency effect of the two models was good. However, compared with the BP neural network prediction model optimized by genetic algorithm, the particle swarm algorithm optimized the support vector machine based moistube irrigation prediction model had higher accuracy. The results of this experiment can provide theoretical support for the exploration and modelling prediction of soil water infiltration under moistube irrigation.

Introduction

The scarcity of freshwater resources has become a threat to agricultural development and the security of the world's food supply due to population growth, climate change, and the loss of agricultural land (Zilov, 2013; Sattari *et al.*, 2020). However, the development of water-saving irrigation can solve the problem of a shortage of fresh water resources and rising food demand (Hamududu and Ngoma, 2020; Zhou *et al.*, 2021; Khamidov, 2019). As a type of water-saving irrigation method, moistube irrigation has the advantages of low energy consumption, high water utilization rate, and enhancement of agricultural output, so it has been widely used and developed (Dirwai *et al.*, 2021). Xue *et al.*, 2013 tested soil water infiltration during moistube irrigation with various pressure heads, and the results revealed that the pressure head had a positive correlation with the cumulative infiltration rate. Zhang *et al.*, 2017 investigated soil water infiltration experiments

with different bulk density under moisture irrigation, and the results showed that the cumulative infiltration rate was negatively correlated with soil bulk density. For silty clay loam and coarse sandy loam, Dirwai *et al.*, 2022 created a geometric empirical model of soil wetting, and the calibration of the model showed that soil texture affected water movement. Zhang *et al.*, 2016 evaluated how clay and clay loam affected soil water infiltration under moisture irrigation. Studies indicated a negative relationship between clay content and the cumulative infiltration rate. Most studies have only investigated the effects of two factors under moisture irrigation.

Back propagation neural networks (abbreviation, BP) have ideal adaptability and fault tolerance, and they are widely used in intelligent computing (Jain, 2010; Jain *et al.*, 1996). However, issues with the computation process, such as delayed convergence and an easy fall into local extremums, will arise, leading to significant mistakes in the outcome (Basheer and Hajmeer, 2000; White, 1989; Embrechts *et al.*, 2014; Christiansen *et al.*, 2010). The genetic algorithm (abbreviation, GA) uses a parallel search mechanism to seek the most ideal results for individuals in the fitness function (Yang and Honavar, 2002; Bekiroglu *et al.*, 2009; Yuen and Chow, 2009). Therefore, the genetic algorithm can find the optimal values of weights and thresholds in the BP neural network, so as to improve the prediction effect of the BP neural network (Leung *et al.*, 2003; Cai *et al.*, 2019). Support vector machine (abbreviation, SVM) is an effective machine learning algorithm proposed on the basis of statistical theory that can solve the problems of small sample, nonlinearity, and high dimensionality (He *et al.*, 2013; Li *et al.*, 2010; Chauhan *et al.*, 2019). The traditional SVM uses the grid search cross-validation method to optimize its parameters, but the subjective factors of this method are greatly affected, and the search and verification process takes a long time. The particle swarm algorithm (abbreviation, PSO) has the advantages of strong guidance, fast convergence speed, and high accuracy, which can find the optimal solution of the support vector machine parameters and improve the prediction accuracy of the model (Kun *et al.*, 2015; Song *et al.*, 2022; Lin *et al.*, 2008). Therefore, the two optimized models are widely used in many fields and disciplines. Liang *et al.*, 2019 investigated the inversion of soil moisture using the GA-BP method, the experiment indicated that the non-linear fitting ability of the model was well developed and the fitting process was stable. Qin and Fan, 2021 researched the Loess Plateau's distinctive curves for predicting soil water. All of the results demonstrated that this method was reliable and universally useful. Based on the PSO-SVM prediction

model, Li *et al.*, 2010 analyzed the erosion characteristics of small watersheds, and Xue *et al.*, 2020 established a freeze-thaw soil evaporation prediction model. The results showed that the GA-BP and PSO-SVM method had a good prediction effect.

There are many influencing factors of soil water infiltration under moistube irrigation. The purpose of this paper is to analyze the influence of multiple factors, and to study and analyze the prediction model of soil water infiltration under the interaction of multiple factors. In this study, soil moisture infiltration data of different bulk density and texture under different pressure heads were obtained through an indoor moistube irrigation infiltration test. The gray correlation analysis method was used to analyze the interaction of multiple factors to determine the input variables of the model, and the BP neural network method optimized by genetic algorithm and the support vector machine method optimized by particle swarm algorithm were used to establish the Kostikov model of soil water infiltration under moistube irrigation. The two models were compared and analyzed to select the best prediction model. The hypothesis of the test is that the PSO-SVM method is more suitable than the BP method for the soil water infiltration model of the moistube irrigation. It is hoped that the results of this experiment can provide a reference and basis for improving the relevant theory of soil water infiltration under moistube irrigation.

Materials and Methods

Experimental equipment

The experiment was performed in the Soil Science Laboratory of the College of Water Conservancy and Engineering, Taiyuan University of Technology, China. A movable bracket, Mariotte bottle, water pipe, moistube pipe, soil box, and other components made up the majority of the experimental apparatus. The movable bracket is an iron bracket with a horizontal top portion and a height adjustment range of around 2m. On the Mariotte bottle, which has a scale marked on it, the change in scale during the test is read to determine the amount of water consumed. The black polyethylene (PE) water pipe, which joins the Mariotte bottle and the moistube pipe, has an inner diameter of 16 mm. The moistube measured 1 m in length, 16 mm in inner diameter, and 1 mm in wall thickness. The soil box is made of plexiglass panels and measures 100 cm × 40 cm × 40 cm (length × width × height), the experimental apparatus is shown in Figure 1. The soil samples utilized

in the experiment were from Shanxi Province's Taiyuan, Datong, and Yuncheng cities. The soil samples were homogeneously mixed and sieved with a 2 mm sieve after air dried and crushed with a stone roller. A laser particle size analyzer was used to determine the soil particle size distribution, and the drying method was used to determine the initial soil water content. The basic physical properties of soil samples are shown in Table 1.

Experimental design and methods

In this paper, the control variable method was used to carry out two sets of experiments, using three different pressure heads of 1m, 1.5m, and 2m were set in both groups. Experiment 1 was the soil water infiltration test, in which soils with bulk densities of 1.20g/cm³, 1.30g/cm³, and 1.40g/cm³ were infiltrated under three different pressure heads. Experiment 2 was a soil moisture infiltration test for loamy sand, sandy loam, and clay loam (LS, SL, and CL) under three different pressure heads, and the bulk densities of the three textures were 1.5 g/cm³, 1.5 g/cm³, and 1.4 g/cm³, respectively. Depending on the needed bulk density, a given number of soil samples were placed into the soil box with a thickness of about 5cm for each layer. The moisture pipe was then installed horizontally on the soil surface when the depth of the soil hit 20cm, and the two ends of the tube went into the holes in the center of both sides of the box. The required soil depth was achieved by filling the soil box with a further 20 cm depth of soil.

The height of the movable stand was modified prior to the start of the test. After testing the 1m pressure head, the bracket was modified to a height of 1m and the Mariotte bottle was inserted. Before the experiment began, the water level in the Mariotte bottle was measured, and the valve was opened to deliver water. When measuring the 1.5m and 2m pressure heads, the procedure outlined above was repeated at the desired height. The valve had been shut down after 120 hours. The water level in the Mariotte bottle was noted every 2 hours during the first 12 hours after the water was first delivered, followed by every 12 hours after that. The cumulative infiltration was calculated from the remaining amount of water in the Mariotte bottle over time. Every experimental treatment was carried out three times.

Data processing and analysis

In this work, the Kostiakov two-parameter model was adopted. This model is one of the many soil water infiltration models proposed according to the basic principle of Darcy's law infiltration, which has the advantages of wide application, high accuracy and easy understanding. And the specific formula is:

$$I = \alpha t^\beta \quad (1)$$

Where I is the cumulative infiltration at any point in time, cm^3 ; α is the infiltration coefficient; β is the infiltration index, which reflects the decay rate of soil infiltration capacity; t is the infiltration time, min.

For the prediction model established in this paper, the accuracy of the model was evaluated by absolute error (AE), relative error (RE), root mean square error (RMSE), and coefficient of determination (R^2), and the specific formulas are:

$$AE_i = |x_i - x'_i| \quad (2)$$

$$RE_i = \frac{|x_i - x'_i|}{x_i} \quad (3)$$

$$RMSE = \sqrt{\frac{\sum_{i=1}^n (x_i - x'_i)^2}{n}} \quad (4)$$

$$R^2 = \frac{\sum_{i=1}^n (x'_i - \bar{x}_i)^2}{\sum_{i=1}^n (x_i - \bar{x}_i)^2} \quad (5)$$

Where x_i is the measured value; x'_i is the predicted value; \bar{x}_i is the average of the measured values; n is the number of samples.

The analysis step for gray correlation

Establish parent and child sequences

Set a number of research objects and call the main sequence of research objects the parent sequence, that is:

$$X_0 = \{X_0(1), X_0(2), \dots, X_0(i)\} \quad (6)$$

Where, $i=1, 2, \dots, n$.

The object being evaluated is a subsequence, that is:

$$X_k = \{X_k(1), X_k(2), \dots, X_k(i)\} \quad (7)$$

Where, $i=1, 2, \dots, n$; $k=0, 1, 2, \dots, n$.

Dimensionless averaging processing of data

Averaging is performed to obtain a new sequence, and the formula is as follows:

$$\widehat{X}_k(i) = \frac{nX_k(i)}{\sum_{i=1}^n X_k(i)} \quad (8)$$

Where, $i=1, 2, \dots, n$; $k=0, 1, 2, \dots, n$.

Determine the correlation coefficient

The degree of correlation between curves can be measured by the size of the curve difference, and the difference between the parent sequence curve and the sub-sequence curve is the correlation coefficient, which is described as follows:

$$L_k(i) = \frac{\Delta_{min} + 0.5\Delta_{min}}{\Delta_k(i) + 0.5\Delta_{max}} \quad (9)$$

$$\Delta_k(i) = |X_0(i) - X_k(i)| \quad (10)$$

$$\Delta_{min} = \min_{1 \leq k \leq M} \{ \min[\Delta_k(i), i = 1, 2, \dots, n] \} \quad (11)$$

$$\Delta_{max} = \max_{1 \leq k \leq M} \{ \max[\Delta_k(i), i = 1, 2, \dots, n] \} \quad (12)$$

Calculate the degree of relevance

The information provided by the correlation coefficient is too scattered and inconvenient to compare, so the correlation coefficient is weighted to obtain the correlation degree. The correlation coefficient determined by combining the points yields the correlation degree R_k , the calculation formula is as follows:

$$R_k = \frac{1}{n} \sum_{i=1}^n L_k(i) \quad (13)$$

Where, $i=1, 2, \dots, n$. The magnitude of the correlation degree R_k can reflect the degree of association between the parent sequence and the subsequence, and the greater the correlation, the closer the relationship. When the general correlation degree is greater than or equal to 0.8, it indicates that the subsequence has a good correlation with the parent sequence; when the correlation degree is between 0.6 and 0.8, the correlation is good; when the correlation degree is less than 0.5, it indicates that the subsequence is essentially not related to the parent sequence.

The genetic algorithm optimizes the BP neural network model

To increase the model's accuracy, the genetic algorithm adjusts the BP neural network's parameters. The GA-BP neural network calculation procedure is primarily separated into three stages: BP neural network structure determination, genetic algorithm optimization of BP neural network weight and threshold, and BP neural network prediction. Figure 2 displays the specific algorithm.

Particle swarm optimization optimizes the support vector machine model

Using the SVM algorithm based on PSO optimization to find the optimal model parameters, which can avoid the problems of large calculations and low accuracy of grid search and cross-validation methods, and the basic operation process is shown in Figure 3.

Results and Discussion

The interaction of multiple factors

The results of the cumulative infiltration are shown in Figure 4(a-c), and the cumulative infiltration at 1.2 g/cm³, 1.3 g/cm³, and 1.4 g/cm³ increased significantly over 120 hours as the pressure head increased from 1m to 2m. However, the difference in cumulative infiltration between soils under different bulk densities was small at 0-12 hours and large at 12-120 hours. With the increase of bulk density from 1.2 g/cm³ to 1.4 g/cm³, the greater the bulk density, the smaller the cumulative infiltration under the pressure head of 1m, 1.5m, and 2m. As the moisture contains nanopores that are uniformly and densely distributed over the moisture surface, during irrigation, the soil water movement approximates line source infiltration. Many researchers have shown that soil bulk density is an important factor that affects soil infiltration capacity. Under the same soil conditions, when the soil bulk density increases, the soil becomes dense and porosity decreases, which results in a decrease of soil infiltration capacity (Dao, 1993; Yang and Zhang, 2011; León *et al.*, 2015; Naglič *et al.*, 2014). The same result was seen in this experiment. As shown in Figure 4(d-f), the cumulative infiltration of loamy sand (LS), sandy loam (SL) and clay loam (CL) increased significantly at 120 hours as the pressure head increased from 1 m to 2 m. At the same time, under the pressure head of 1m, 1.5m and 2m, the cumulative infiltration of different soil textures in 120 hours was loamy sand (LS) > sandy loam (SL) > clay loam (CL). The cumulative infiltration of loamy sand (LS) is the

largest at a high pressure head of 2m, and the cumulative infiltration of clay loam (CL) is the lowest at a low pressure head of 1m. The cumulative infiltration was greater for coarse-textured soil and less for fine-textured soil under moisture irrigation.

As shown in Figure 5(a-c), the infiltration rates of the moisture under different pressure heads and soil bulk densities increased rapidly during the first 12 hours, then decreased over the next 12–36 hours, and it stabilized after 48 hours. For different pressure heads, the infiltration rates of the moisture ranked as 2m > 1.5m > 1m with significant differences among them. Soil bulk densities ranked as 1.20 g/cm³ > 1.30 g/cm³ > 1.40 g/cm³ with significant differences among them under the pressure head of 2m and 1.5m. Under the 1m pressure head, the infiltration rate of the moisture for 1.30 g/cm³ was close to 1.40 g/cm³ with no significant difference between them, both were significantly lower than 1.20 g/cm³. As shown in Figure 5(d-f), the infiltration rate of the moisture under different soil textures increased rapidly over 0–12 hours, then decreased over 12–24 hours, and levelled off after 36 hours. For different soil textures, the infiltration rates of the moisture ranked as loamy sand (LS) > sandy loam (SL) > clay loam (CL) with significant differences among them. As the pressure head increases, the infiltration rates of the moisture ranked as loamy sand (LS) > sandy loam (SL) > clay loam (CL) with among them. The infiltration rates of the moisture increased rapidly at the beginning of irrigation, then decreased and remained at a stable level as time went on. The potential reason for this was that nano-pores at the surface of the moisture could not be completely opened when the moisture began to irrigate, and the discharge of moisture was unstable until the vast majority of nano-pores were opened under the water pressure. There was an induction period that probably occurred within 12 hours of the start of moisture irrigation, and the discharge of moisture remained stable after 36–48 hours of irrigation. In addition, the water potential difference between inside and outside of the moisture is large when irrigation begins, and the discharge of the moisture is higher. As irrigation time went on, the water potential difference became smaller, and the discharge was gradually stable (Qiu *et al.*, 2015; Niu *et al.*, 2017). The difference between the time needed to develop the stable infiltration rate of moisture may have been related to the pressure head, soil bulk density, soil texture, soil initial water content, and different test conditions.

Determination of input and output parameters

The Kostiakov infiltration model was applied in this study. The infiltration coefficient and cumulative infiltration were quantitatively close at the end of the first unit period. The level of soil infiltration capacity degradation was demonstrated by the infiltration index. Both the parameters α and β are affected by the pressure head, soil density, soil texture and initial water content. The higher the volumetric water content of the soil, the lower the water suction and the slower the rate of soil water infiltration, resulting a decrease in the magnitude of the parameters α and β of the Kostiakov infiltration model. The soil was denser, the soil porosity was smaller, the connectedness was worse, and the infiltration flux per unit area was lower due to the bulk density of the soil being higher. As a result, the Kostiakov infiltration model's parameters α and β were reduced. The percentage content of clay, silt, and sand particles in the soil is typically used to characterize the soil texture, since soil texture is the ratio of soil solid phase particles at each grain level. The amount of clay in the soil was larger, the soil particles were smaller, and the adsorption capacity was greater, which caused a drop in both the water flux and the pace at which water seeped into the soil. In turn, the Kostiakov infiltration model's parameters α and β had lower values.

The influencing factors of soil water infiltration under moisture irrigation include the pressure of the water source and the initial moisture content, bulk density, texture that characterize the basic physical and chemical properties of soil. Since the influence of each factor on the model parameters cannot be quantified, the correlation between the physical and chemical parameters and the model parameters cannot be judged. Therefore, the gray correlation degree of each influence factor is calculated by using gray correlation theory. The factors are ranked, and the influence degree of each factor on the parameters of the Kostiakov infiltration model is quantified, which provides a basis for a reasonable selection of input factors of the prediction model. The correlation degree between the parameters of Kostiakov infiltration model α and β and pressure head, soil bulk density, soil texture, and soil initial moisture content is calculated, and the results are shown in Table 2. The relevance of parameter α is sorted as: $X_1 > X_2 = X_6 > X_3 > X_4 > X_5$, and the relevance of parameter β is sorted as: $X_2 > X_6 > X_1 > X_3 > X_4 > X_5$. The correlation degree of the six impact factors was greater than 0.6, and the correlation degree was good. Because the soil sample was air-dried soil, the initial water content was relatively low, resulting in a low ranking. Finally, six indexes, namely pressure head, soil

bulk density, clay content, silt content, sand content, and initial water content, were selected as input variables, and the infiltration coefficient and infiltration index were selected as output variables, so as to establish the prediction model of Kostiakov soil water infiltration under moisture irrigation.

The results of the predictive models

A total of 68 sets of data were gathered for this investigation. The training dataset and verification dataset were split into two groups according to a 4:1 ratio, with 54 sets of data in the training set and 14 sets in the verification set. There were five main indicators affecting soil water infiltration under moisture irrigation, and the target parameters were the infiltration coefficient and infiltration index of the Kostiakov infiltration model. The GA-BP model and PSO-SVM model were used to predict the parameters α and β , and the model effect and accuracy were analyzed for the predicted value and measured value of the model.

The effect of the GA-BP prediction model

In this study, the GA-BP prediction model's input layer was 6, the output layer was 2, and the hidden layer was 8. The evolutionary algorithm used in this study had a population size of 10, a maximum of 120 iterations, a crossover probability of 0.4, and a mutation probability of 0.02.

The GA-BP model was used to forecast the Kostiakov infiltration model parameters α and β . The training and validation impacts were assessed based on the consistency of the model's anticipated and measured values. The consistency was stated as the slope (k) and coefficient of determination (R^2) of the linear equation produced from the model's predicted and measured values, and the results are displayed in Figure 6. For the training set, the slopes (k) of the parameters α and β were 0.9506 and 0.9566, respectively, and their coefficients of determination (R^2) were 0.9207 and 0.9486, respectively. For the validation set, the slopes (k) of the parameters α and β were 0.9814 and 1.003, respectively, and their coefficients of determination (R^2) were 0.9868 and 0.9739, respectively. The slope (k) and coefficient of determination (R^2) of the parameters and were extremely close to one, demonstrating that the projected values of the GA-BP model training set samples are consistent with the measured values.

The effect of the PSO-SVM prediction model

In this paper, the population size of the particle swarm algorithm was set to 30, the maximum number of iterations was 120, and the optimal values of the penalty coefficient C of the two parameters, the kernel parameter g , and the width of the insensitive loss function ε are obtained according to the set accuracy conditions. The optimal result of the parameter α : C was 81.26, g was 2.69, ε was 0.013. The optimal result of the parameter β : C was 79.30, g was 19.87, ε was 0.034.

The parameters α and β of the Kostikov infiltration model were predicted using the PSO-SVM model, and the slope (k) and coefficient of determination (R^2) expressed in agreement were shown in Figure 7. For the training set, the slopes (k) of the parameters α and β were 0.9686 and 0.9712, respectively, and their coefficients of determination (R^2) were 0.9902 and 0.9833, respectively. For the validation set, the slopes (k) of the parameters α and β were 0.9894 and 0.9736, respectively, and their coefficients of determination (R^2) were 0.9947 and 0.9860, respectively. It can be seen that the slope (k) and coefficient of determination (R^2) of the parameters α and β were very close to 1, indicating that the predicted values of the training set samples of the PSO-SVM model were in good agreement with the measured values.

Comparison of predictive models

According to the error results between the predicted value and the measured value of the model, the prediction accuracy of the training set and the validation set was evaluated. The error results were displayed by the statistical indicators AE, RE, and RMSE, and the results are shown in Table 3. Under the GA-BP prediction model, the AE mean and RE mean values for the training set for parameter α were 0.0076 and 0.0663, respectively, and the verification set were 0.0059 and 0.0481, respectively. For parameter β , the AE mean and RE mean of the training set were 0.0221 and 0.0241, respectively, and the average values of the validation set were 0.0192 and 0.0221, respectively. From the results, the error statistical index of parameter α and β were less than 6.6%. Under the PSO-SVM prediction model, the AE mean and RE mean values of the training set for parameter α were 0.0062 and 0.0549, respectively, and the verification set was 0.0055 and 0.0461, respectively. For parameters β , the AE mean and RE mean of the training set were 0.0078 and 0.0088, respectively, and the verification set was 0.0076 and 0.0086, respectively. From the results, the error statistical indicators of parameter α

and β were less than 5.5%. Under the GA-BP prediction model and PSO-SVM prediction model, the error of the validation set was smaller than that of the training set, and the value of RMSE was that the result of the validation set was greater than that of the training set. This showed that the GA-BP neural network prediction model and PSO-SVM prediction had high accuracy.

According to the consistency of the effect plots of the two prediction models, the slope (k) and coefficient of determination (R^2) of the parameters α and β were very close to 1, indicating that the GA-BP prediction model and the PSO-SVM prediction model have strong prediction effects. According to the error analysis of the predicted values and measured values of the parameters α and β , it can be seen that the accuracy of the PSO-SVM prediction model was 0.83 times higher than that of the GA-BP prediction model. Therefore, the PSO-SVM prediction model of soil water infiltration under moisture irrigation established in this paper has higher accuracy.

Model application analysis

There are numerous models of soil water infiltration, with the Kostiakov model being frequently employed because of its simple structure, easy calculation, and lower criteria. Based on the measured data, Hasan *et al.*, 2015, Magnus *et al.*, 2014, O'Brien *et al.*, 2014 all created the Kostiakov model of soil water infiltration, and the findings revealed that the model was in accordance with the cumulative infiltration value. Utin and Oguike, 2018 developed model of soil moisture infiltration for various soil types, and the results showed that the Kostiakov model performance exceeded the Philip model for soils derived from sandstone and alluvial soils. Sun *et al.*, 2019 investigated soil water infiltration under moisture irrigation and found that Kostiakov's infiltration model was compatible with a correlation between cumulative infiltration amount and infiltration time. Zhang *et al.*, 2018 investigated the effects of different pressure heads and moisture burial depths on the cumulative infiltration of soil water, and obtained results indicating that the changes of the cumulative infiltration of moisture irrigation were consistent with the Kostiakov model. In this study, the Kostiakov infiltration model under moisture irrigation was established with the cumulative infiltration of different pressure heads, soil bulk density and soil texture, and the results were consistent with the conclusions of the previous studies described above. Therefore, the cumulative infiltration under moisture irrigation according to different influencing factors is in line with the Kostiakov infiltration

model.

The drawbacks of conventional BP neural networks, which have a high reliance on weights and thresholds, are resolved, and the ability to solve problems is improved, by combining genetic algorithms and BP neural networks. Similarly, particle swarm optimization has the characteristics of strong guidance, fast convergence speed, and high solution accuracy, which can improve the algorithm recognition accuracy of the support vector machine and optimize the prediction effect of the model. In this study, the measured datasets of soil moisture infiltration under moisture irrigation with different pressure heads, bulk densities and soil textures were obtained according to the indoor soil box experiment. Then, according to the pressure head, bulk density, clay content, silt content, sand content and initial moisture content, the prediction of Kostiakov's infiltration model was carried out using the BP neural network method optimized by a genetic algorithm and the support vector machine method of particle swarm optimization. And the accuracy and prediction effect were good, and the accuracy of PSO-SVM was higher. Kun *et al.*, 2015 established a hyperspectral inversion model of soil organic matter content. Ming *et al.*, 2021 explored the prediction methods of soil moisture. The results of multiple models were comparatively analyzed, and the results showed that the accuracy of the PSO-SVM prediction model was higher, which is consistent with the results of this paper. Therefore, the GA-BP and PSO-SVM prediction methods are widely used, and good prediction accuracy and prediction effect can be achieved under different influencing factors and experimental conditions of soil water infiltration under moisture irrigation.

Conclusions

According to the influencing factors of soil water infiltration under moisture irrigation, the gray correlation theory was used to determine the input variables of the model. The two parameters of the Kostiakov model of soil water infiltration were taken as the output variables. Then, the BP neural network method improved by a genetic algorithm and the support vector machine method optimized by the particle swarm algorithm. Finally, the soil water infiltration prediction model under moisture irrigation were established. Whether it was a training set or a validation set, both predictive models had good prediction effects. In addition, the PSO-SVM model established in this paper has higher accuracy than the GA-BP neural network model. The results showed that the predictive PSO-SVM

model for soil moisture infiltration under micro-irrigation was more suitable in small-sample tests.

References

- Basheer, I. A. & Hajmeer, M. (2000). Artificial neural networks: fundamentals, computing, design, and application. *Journal of Microbiological Methods* 43(1): 3-31.[http://dx.doi.org/10.1016/S0167-7012\(00\)00201-3](http://dx.doi.org/10.1016/S0167-7012(00)00201-3)
- Bekiroglu, S., Dede, T. & Ayvaz, Y. (2009). Implementation of different encoding types on structural optimization based on adaptive genetic algorithm. *Finite elements in analysis design* 45(11): 826-835.<http://dx.doi.org/10.1016/j.finel.2009.06.019>
- Cai, X., Chen, J., Ji, Y., Liu, M. & Liu, W. (2019). Structural Optimization and Performance Prediction of a Compact Flotation Unit Using GA-BP Neural Network with Computational Fluid Dynamics Simulation. *Environmental Engineering Science* 36(9): 1185-1198.<http://dx.doi.org/10.1089/ees.2018.0327>
- Chauhan, V. K., Dahiya, K. & Sharma, A. (2019). Problem formulations and solvers in linear SVM: a review. *Artificial Intelligence Review* 52(2): 803-855.<http://dx.doi.org/10.1007/s10462-018-9614-6>
- Christiansen, M. H., Kelly, M. L., Shillcock, R. C. & Greenfield, K. (2010). Impaired artificial grammar learning in agrammatism. *Cognition* 116(3): 382-393.<http://dx.doi.org/10.1016/j.cognition.2010.05.015>
- Dao, T. H. (1993). Tillage and winter wheat residue management effects on water infiltration and storage. *Soil Science Society of America Journal* 57(6): 1586-1595.<http://dx.doi.org/10.2136/sssaj1993.03615995005700060032x>
- Dirwai, T. L., Mabhaudhi, T., Kanda, E. K. & Senzanje, A. (2021). Moisture irrigation technology development, adoption and future prospects: A systematic scoping review. *Heliyon* 7(2): e06213.<http://dx.doi.org/10.1016/j.heliyon.2021.e06213>
- Dirwai, T. L., Senzanje, A. & Mabhaudhi, T. (2022). Development and validation of a model for soil wetting geometry under Moisture Irrigation. *Scientific Reports* 12(1): 1-13.<http://dx.doi.org/10.1038/s41598-022-06763-x>
- Embrechts, M. J., Rossi, F., Schleif, F. M. & Lee, J. A. (2014). Advances in artificial neural networks,

machine learning, and computational intelligence (ESANN 2013). *Neurocomputing* 141: 1-2. <http://dx.doi.org/10.1016/j.neucom.2014.03.002>

Hamududu, B. H. & Ngoma, H. (2020). Impacts of climate change on water resources availability in Zambia: implications for irrigation development. *Environment, Development and Sustainability* 22(4): 2817-2838. <http://dx.doi.org/10.1007/s10668-019-00320-9>

Hasan, M., Chowdhury, T., Drabo, M., Kassu, A. & Glenn, C. (2015). Modeling of Infiltration Characteristics by Modified Kostiaikov Method. *Journal of Water Resource Protection* 7(16): 1309-1317. <http://dx.doi.org/10.4236/jwarp.2015.716106>

He, C., Xing, J. C., Zhu, R. D., Li, J. L., Yang, Q. L., Xie, L. Q. & Ieee (2013). A New Model for Software Defect Prediction Using Particle Swarm Optimization and Support Vector Machine. In *25th Chinese Control and Decision Conference (CCDC)*, 4106-4110 Guiyang, PEOPLES R CHINA.

Jain, A. K., Mao, J. & Mohiuddin, K. M. (1996). Artificial Neural Networks. *Computer* 29(3): 31-44. <http://dx.doi.org/10.1109/2.485891>

Jain, L. C. (2010). Advances in design and application of neural networks. *Neural Computing Applications* 19(2): 167-168. <http://dx.doi.org/10.1007/s00521-010-0345-0>

Khamidov, M. (2019). Water-saving irrigation technology as a way of using water resources sustainably in the Khorezm oasis. *International Journal of Innovative Technology Exploring Engineering* 9(2): 851-856. <http://dx.doi.org/10.35940/ijitee.B6718.129219>

Kun, T., Qianqian, Z., Qian, C. & Peijun, D. (2015). Hyperspectral Retrieval Model of Soil Organic Matter Content Based on Particle Swarm Optimization-Support Vector Machines. *Earth Science(Journal of China University of Geosciences)* 40(8): 1339-1345. <http://dx.doi.org/10.3799/dqkx.2015.115>

León, J., Echeverría, M., Martí, C. & Badía, D. (2015). Can ash control infiltration rate after burning? An example in burned calcareous and gypseous soils in the Ebro Basin (NE Spain). *Catena* 135: 377-382. <http://dx.doi.org/10.1016/j.catena.2014.05.024>

Leung, F., Lam, H. K., Ling, S. H. & Tam, P. (2003). Tuning of the structure and parameters of a neural network using an improved genetic algorithm. *IEEE Trans Neural Netw* 14(1): 79-88. <http://dx.doi.org/10.1109/TNN.2002.804317>

- Li, Y. K., Tian, Y. J., Ouyang, Z. Y., Wang, L. Y., Xu, T. W., Yang, P. L. & Zhao, H. X. (2010). Analysis of soil erosion characteristics in small watersheds with particle swarm optimization, support vector machine, and artificial neuronal networks. *Environmental Earth Sciences* 60(7): 1559-1568.<http://dx.doi.org/10.1007/s12665-009-0292-1>
- Liang, Y. J., Ren, C., Wang, H. Y., Huang, Y. B. & Zheng, Z. T. (2019). Research on soil moisture inversion method based on GA-BP neural network model. *International Journal of Remote Sensing* 40(5-6): 2087-2103
- Lin, S. W., Ying, K. C., Chen, S. C. & Lee, Z. J. (2008). Particle swarm optimization for parameter determination and feature selection of support vector machines. *Expert Systems with Applications* 35(4): 1817-1824.<http://dx.doi.org/10.1016/j.eswa.2007.08.088>
- Magnus, Igboekwe, U., Ruth & Adindu, U. (2014). Use of Kostiakov's Infiltration Model on Michael Okpara University of Agriculture, Umudike Soils, Southeastern, Nigeria. *Journal of Water Resource Protection*.<http://dx.doi.org/10.4236/jwarp.2014.610083>
- Ming, X., Bo, W., Juan, L., Cihao, C., Minhui, H. & Lin-xin, Z. (2021). Forecast Method of Soil Moisture Based on Improved BP Neural Network and Support Vector Machine. *Chinese Journal of Soil Science* 52(4): 793-800.<http://dx.doi.org/10.19336/j.cnki.trtb.2020052501>
- Naglič, B., Kechavarzi, C., Coulon, F. & Pintar, M. (2014). Numerical investigation of the influence of texture, surface drip emitter discharge rate and initial soil moisture condition on wetting pattern size. *Irrigation science* 32(6): 421-436.<http://dx.doi.org/10.1007/s00271-014-0439-z>
- Niu, W., Zhang, M., Xu, J., Zou, X., Zhang, R. & Li, Y. (2017). Prediction methods and characteristics of flow for Moistube. *Transactions of the CSAM* 48(6): 217-224.<http://dx.doi.org/10.6041/j.issn.1000-1298.2017.06.028>
- O'Brien, W. L., Jia, J., Dong, Q. Y., Callcott, T. A., Miyano, K. E., Ederer, D. L., Mueller, D. R. & Kao, C. C. (2014). Evaluation on backstepping method of infiltration parameters of soil water under furrow irrigation based on the software SRF. *Agricultural Research in the Arid Areas* 32(4): 59-64.<http://dx.doi.org/10.1103/PhysRevB.47.140>
- Qin, W. & Fan, G. (2021). Estimating parameters for the Van Genuchten model from soil physical-chemical properties of undisturbed loess-soil. *Earth Science Informatics* (3): 14.<http://dx.doi.org/10.1007/s12145-020-00503-3>

- Qiu, Z. N., Jiang, P. F. & Xiao, J. (2015). Experimental Study on Influence of Water Temperature on Outflows of Low Pressure Moistube. *Water Saving Irrigation* 3: 12–14
- Sattari, M. T., Mirabbasi, R., Dolati, H., Sureh, F. S. & Ahmad, S. (2020). Investigating the Effect of Managing Scenarios of Flow Reduction and Increasing Irrigation Water Demand on Water Resources Allocation Using System Dynamics (Case Study: Zonouz Dam, Iran). *Tekirdag Ziraat Fakultesi Dergisi* 17(3): 406-421.<http://dx.doi.org/10.33462/jotaf.703167>
- Song, Z. B., Liu, S. R., Jiang, M. Y. & Yao, S. L. (2022). Research on the Settlement Prediction Model of Foundation Pit Based on the Improved PSO-SVM Model. *Scientific Programming* 2022.<http://dx.doi.org/10.1155/2022/1921378>
- Sun, G., Li, Y., Liu, X., Cui, N., Gao, Y. & Yang, Q. (2019). Effect of Moistube Fertigation on Infiltration and Distribution of Water-Fertilizer in Mixing Waste Biomass Soil. *Sustainability* 11.<http://dx.doi.org/10.3390/su11236757>
- Utin, U. E. & Oguike, P. C. (2018). Evaluation of Philip's and Kostiaikov's Infiltration Models on Soils Derived from three Parent Materials in Akwa Ibom State, Nigeria. *The Journal of Scientific Engineering Research*
- White, H. (1989). Learning in Artificial Neural Networks: A Statistical Perspective. *Neural Computation* 1(4): 425-464.<http://dx.doi.org/10.1162/neco.1989.1.4.425>
- Xue, W. L., Niu, W. Q., Zhang, J., Zhe-Guang, W. U. & Luo, C. Y. (2013). Effects of Hydraulic Head on Soil Water Movement under Moistube-irrigation. *Journal of Irrigation Drainage* 32(6): 7-11.<http://dx.doi.org/10.7631/j.issn.1672-3317.2013.06.002>
- Xue, X., Junfeng, C., Xiuqing, Z., Jing, X., Xiaoyan, Z., Xinyu, D. & Yizhao, W. (2020). Freeze-Thaw Soil Evaporation Forecast Model Based on PCA-PSO-SVM. *Water Saving Irrigation* (1): 61-65.<http://dx.doi.org/10.3969/j.issn.1007-4929.2020.01.014>
- Yang, J. & Honavar, V. (2002). Feature subset selection using a genetic algorithm. *IEEE Intelligent Systems Their Applications* 13(2): 44-49.<http://dx.doi.org/10.1109/5254.671091>
- Yang, J. L. & Zhang, G. L. (2011). Water infiltration in urban soils and its effects on the quantity and quality of runoff. *Journal of soil sediments* 11(5): 751–761.<http://dx.doi.org/10.1007/s11368-011-0356-1>
- Yuen, S. & Chow, C. (2009). A Genetic Algorithm That Adaptively Mutates and Never Revisits. *IEEE*

Transactions on Evolutionary Computation 13(2): 454-472.<http://dx.doi.org/10.1109/TEVC.2008.2003008>

Zhang, G., Shen, L. & Guo, Y. (2016). Effect of Soil Structure on Water Infiltration under Moistube Irrigation. *Journal of Irrigation Drainage* 35(7): 35-38.<http://dx.doi.org/10.13522/j.cnki.gggs.2016.07.006>

Zhang, G., Shen, L. & Guo, Y. (2017). Effect of pressure heads and soil bulk density on water infiltration under moistube irrigation. *Agricultural Research in the Arid Areas* 35(4): 67-73.<http://dx.doi.org/10.7606/j.issn.1000-7601.2017.04.11>

Zhang, S., Guo, X., Bi, Y., Lei, T. & Lei, M. (2018). Effects of Tube Depth and Pressure Head on Soil Water Cumulative Infiltration under Moistube-irrigation. *Water Saving Irrigation* (3): 19-22.<http://dx.doi.org/10.3969/j.issn.1007-4929.2018.03.005>

Zhou, X., Zhang, Y., Sheng, Z., Manevski, K. & Yang, Y. (2021). Did water-saving irrigation protect water resources over the past 40 years? A global analysis based on water accounting framework. *Agricultural Water Management* 249(C): 106793.<http://dx.doi.org/10.1016/j.agwat.2021.106793>

Zilov, E. J. W. R. (2013). Water resources and the sustainable development of humankind: International cooperation in the rational use of freshwater-lake resources: Conclusions from materials of foreign studies. *Water Resources* 40(1): 84-95.<http://dx.doi.org/10.1134/S0097807812030116>

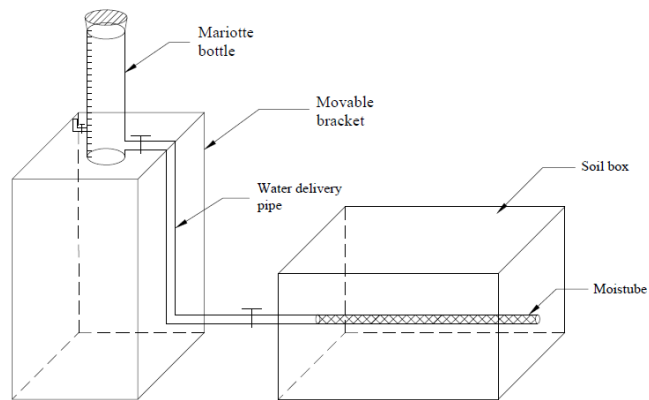


Figure 1. Schematic illustration of the soil box test device.

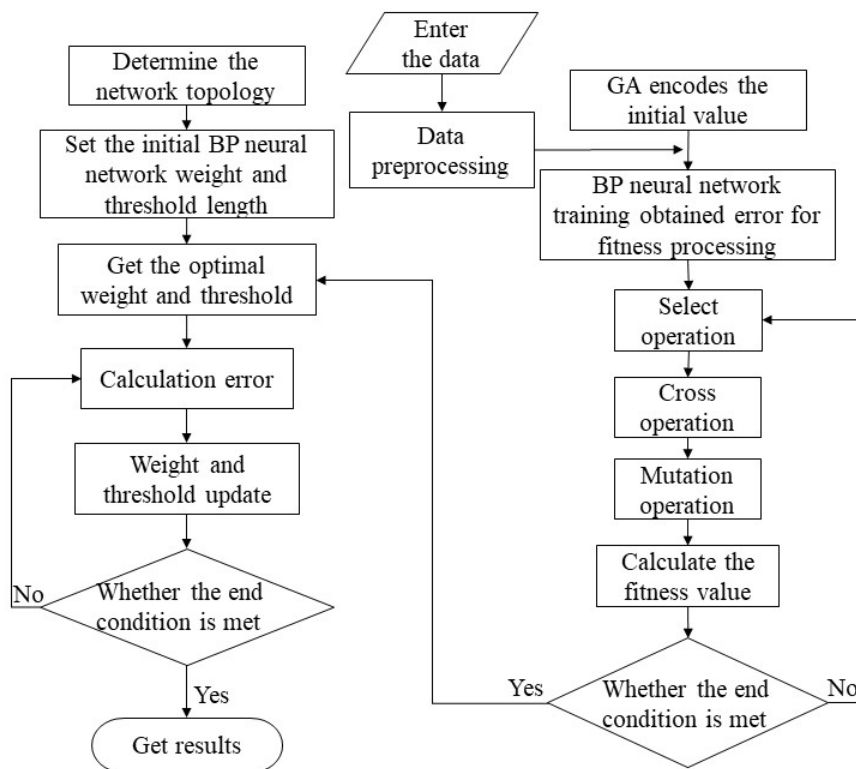


Figure 2. The GA-BP neural network flowchart.

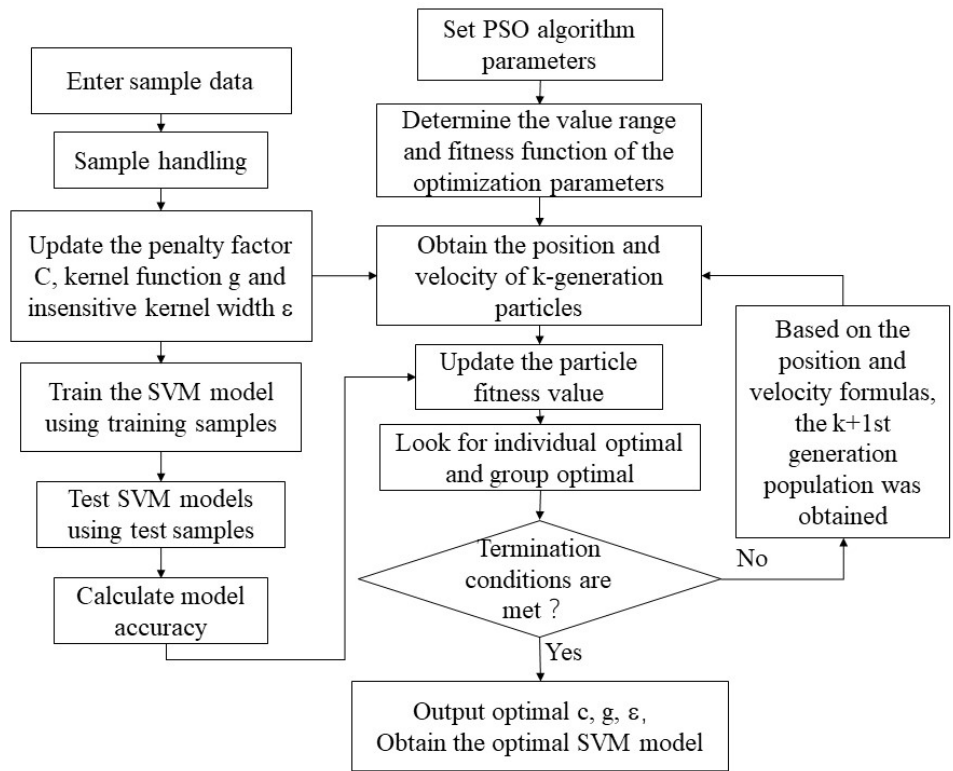


Figure 3. The PSO-SVM neural network flowchart.

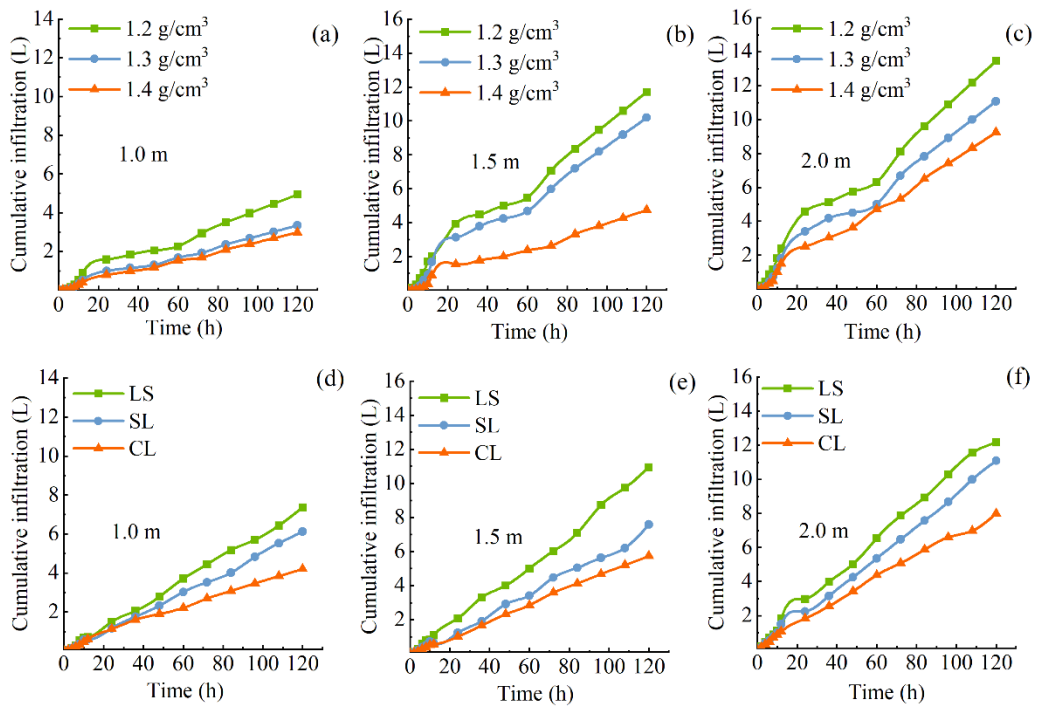


Figure 4. Cumulative infiltration with different pressure heads, bulk density, and texture.

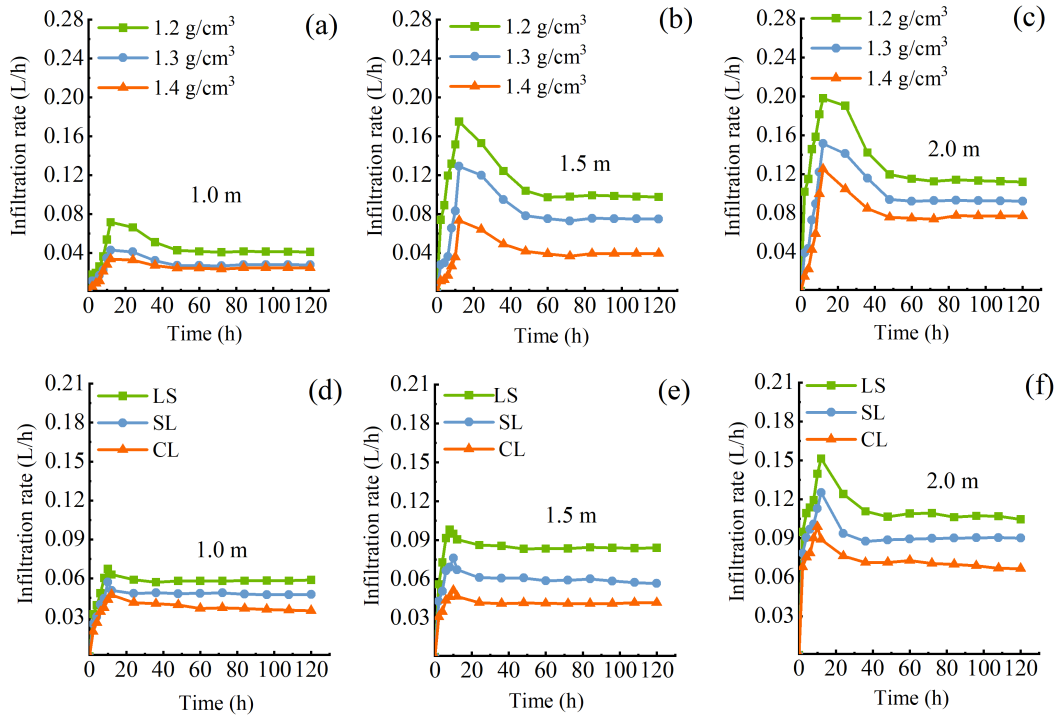


Figure 5. The infiltration rate of different pressure heads, bulk density, and texture.

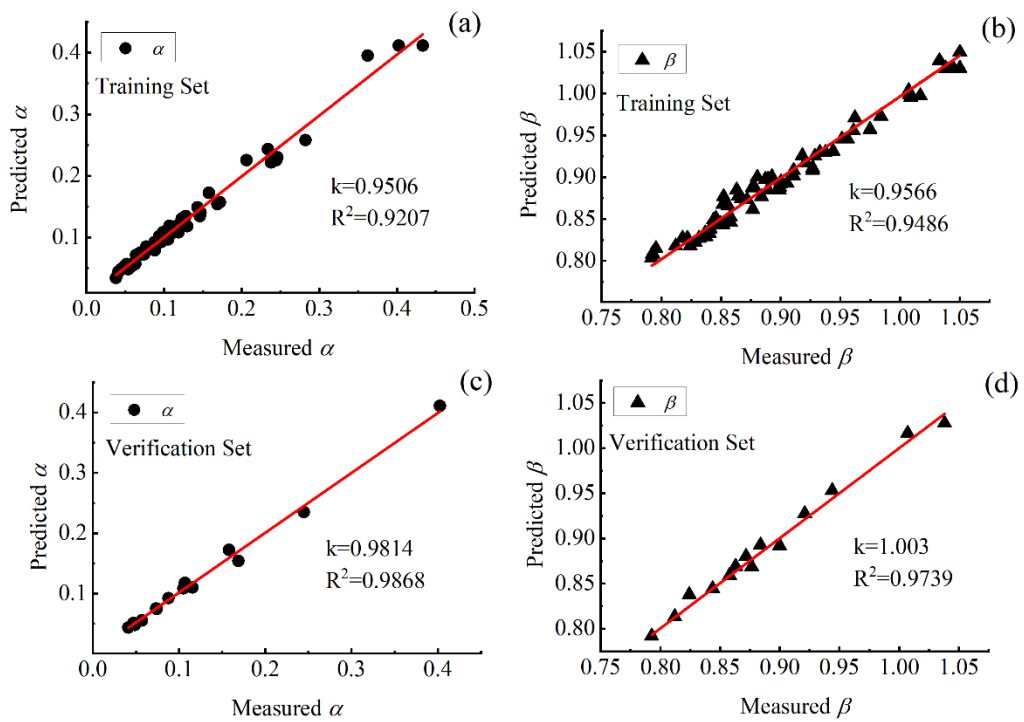


Figure 6. Prediction results of parameters under the GA-BP model.

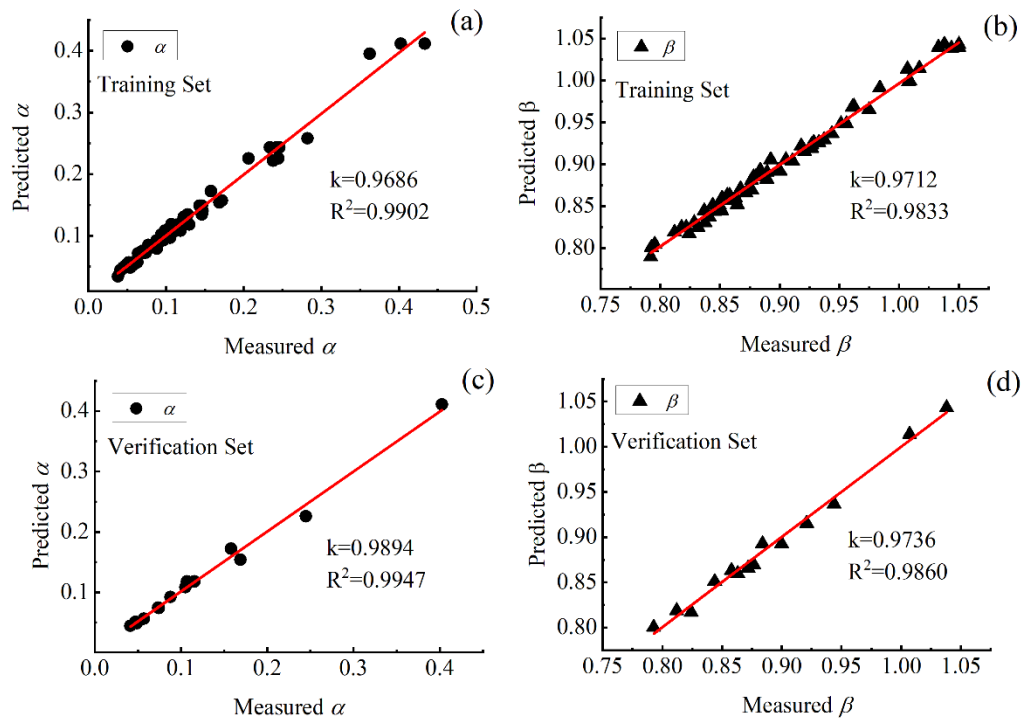


Figure 7. Prediction results of parameters under the PSO-SVM model.

Table 1. Basic physical properties of the tested soils.

Soil Texture	Bulk Density (g/cm ³)	Initial water content (%)	Particle Size (mm)		
			0~0.002	0.002~0.02	0.02~2.00
Clay loam	1.20, 1.30, 1.40	2.26	23.30	40.58	36.12
Loamy sand	1.5	2.12	5.20	7.32	87.48
Sandy loam	1.5	2.37	12.31	25.24	62.45
Clay loam	1.4	2.44	20.43	43.25	36.32

Table 2. Calculation of the correlation of model parameters α and β with the impact factor.

factors	Pressure head (X1)	Bulk density(X2)	clay content(X3)	silt content(X3)	sand content(X4)	initial water content (X5)
α	0.808	0.792	0.777	0.768	0.749	0.792
β	0.697	0.937	0.695	0.650	0.649	0.833

Table 3. The accuracy results of the two predictive models.

Methods	Performance		Parameter α		Parameter β	
			Training set	Validation set	Training set	Validation set
GA-BP	AE	Max	0.0338	0.0147	0.0497	0.0237
		Min	0.0018	0.0005	0.0006	0.0007
		Mean	0.0076	0.0059	0.0221	0.0192
	RE	Max	0.1161	0.0953	0.0566	0.0379
		Min	0.0094	0.0069	0.0006	0.0008
		Mean	0.0663	0.0481	0.0241	0.0221
	RMSE		0.0011	0.0011	0.0012	0.0021
PSO-SVM	AE	Max	0.0179	0.0175	0.0267	0.0140
		Min	0.0008	0.0005	0.0023	0.0043
		Mean	0.0062	0.0055	0.0078	0.0076
	RE	Max	0.1216	0.0933	0.0320	0.0163
		Min	0.0034	0.0133	0.0027	0.0050
		Mean	0.0549	0.0461	0.0088	0.0086
	RMSE		0.0010	0.0010	0.0010	0.0019